Two-Photon Absorption Properties of Dehydrobenzo[12]annulenes and Hexakis(phenylethynyl)benzenes: Effect of Edge-Linkage

ARTICLE *in* CHEMPHYSCHEM · DECEMBER 2007

Impact Factor: 3.42 · DOI: 10.1002/cphc.200700555 · Source: PubMed

9 AUTHORS, INCLUDING:

Liudmil Antonov
Bulgarian Academy of Sciences
99 PUBLICATIONS **1,586** CITATIONS
SEE PROFILE

Kazukuni Tahara
Osaka University
76 PUBLICATIONS **2,384** CITATIONS
SEE PROFILE

Yoshito Tobe
Osaka University
281 PUBLICATIONS **4,922** CITATIONS
SEE PROFILE

DOI: 10.1002/cphc.200700555

Two-Photon Absorption Properties of Dehydrobenzo[12]annulenes and Hexakis(phenylethynyl)benzenes: Effect of Edge-Linkage

Kenji Kamada,*[a] Liudmil Antonov,[a, b] Satoru Yamada,[c] Koji Ohta,[a] Takashi Yoshimura,[d] Kazukuni Tahara,[d] Akiko Inaba,[d] Motohiro Sonoda,[d] and Yoshito Tobe[d]

Two-photon absorption (TPA) properties of two trefoil-shaped compounds with different edge linkages—tris(hexadehydrotribenzo[12]annulene) and tris(tetradehydrotribenzo[12]annulene)—and three asterisk-shaped compounds having no edge-linkage—hexakis(phenylethynyl)benzenes—are investigated experimentally by the open-aperture Z-scan and TPA-induced fluorescence methods with wavelength tuneable femtosecond pulses. The compound with ethynylene edge-linkage exhibits the most intense TPA (the maximal TPA cross section is 1300 ± 170 GM at 572 nm where 1 GM = 10^{-50} cm^4 s molecule^{-1} photon^{-1}). The TPA activity of the compounds is primarily explained in terms of the planarity of the molecules in relation with the type of edge-linkage.

1. Introduction

Carbon allotropes are surprisingly varied in their mechanical, thermal, electrical, and optical properties depending on their structure. Diamond, graphite, fullerenes, and carbon nanotubes, are all carbon allotropes. Among these, graphite has an infinite two-dimensional carbon network and forms a macromolecule with an extended π-conjugation over the molecular plane. Currently artificial extensions of the graphite carbon-network, such as graphyne and graphdiyne, are the subject of interest among chemists and physicists because of their unexplored material properties.[1–3] Graphyne and graphdiyne consist of phenyl rings on hexagonal lattice points interconnected by ethynylene and butadiynylene groups, respectively. The minimum repeating unit for graphyne is hexadehydrotribenzo[12]annulene ([12]DBA, **1** in Scheme 1) and that for graphdiyne is dodecadehydrotribenzo[18]annulene ([18]DBA). Molecules built with these triangular subunits have been investigated extensively in terms of their structural, optical, and nonlinear optical properties.[4–12]

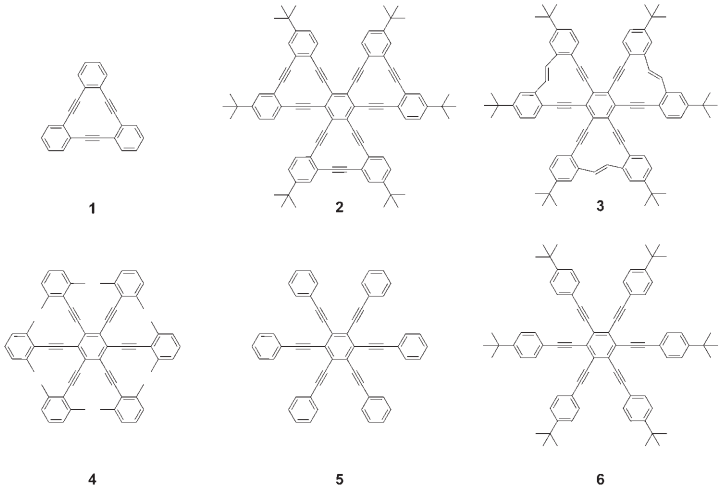

Scheme 1. Structures of the compounds studied (DBAs: **1–3**, HPEBs: **4–6**)

Very recently, Bhaskar and co-workers reported two-photon absorption (TPA) properties of the compounds built with the [18]DBA subunit.[12] They found that the [18]DBA compounds exhibit relatively large TPA cross sections, especially for the trefoil-shaped trimer of [18]DBA. The peak cross section of the trimer is reported to be 1350 GM at 770 nm, (where 1 GM = 10^{-50} cm^4 s molecule^{-1} photon^{-1}) which is a very large value for hydrocarbons without strong donor or acceptor groups, except for singlet diradical species.[13] The TPA cross section decreases when the number of [18]DBA subunits is small, howev-

[a] *Dr. K. Kamada, Prof. L. Antonov, Dr. K. Ohta*
Photonics Research Institute
National Institute of Advanced Industrial Science and Technology (AIST)
Ikeda, Osaka 563-8577 (Japan)
Fax: (+81) 72-751-9637
E-mail: k.kamada@aist.go.jp

[b] *Prof. L. Antonov*
Institute of Organic Chemistry, Bulgarian Academy of Sciences
Acad. G. Bonchev str. bl. 9, Sofia 1113 (Bulgaria)

[c] *Dr. S. Yamada*
Department of Chemistry, Graduate School of Science
Osaka University, Toyonaka, Osaka 560-0043 (Japan)

[d] *T. Yoshimura, Prof. K. Tahara, A. Inaba, Prof. M. Sonoda, Prof. Y. Tobe*
Division of Frontier Materials Science
Graduate School of Engineering Science, Osaka University
Toyonaka, Osaka 560-8531 (Japan)

er this depends on the combination of the subunits. They concluded that not high chromophore density but high symmetry is the determining factor for high TPA cross section for their systems.

Their finding is very interesting from a structure-property relationship viewpoint. However, it is still not clear why "high symmetry" gives rise to the large TPA cross section. For this, two possible mechanisms can be considered. One is increasing planarity of the molecule by interconnecting the peripheral phenyl rings located at apexes of the hexagon envelope. Another is the electronic coupling between the π-conjugated path along the edge of the hexagon and the path along the diametric direction. These two mechanisms are related to the π-conjugation linkage at the hexagon edges. Thus, we focus on the effect of edge-linkage on the TPA properties. Herein, we report the TPA properties of the [12]DBA and the related compounds investigated by the open-aperture Z-scan and two-photon-induced fluorescence (TPIF) methods with a femtosecond light source. The compounds (Scheme 1) studied are two trefoil-shaped [12]DBA trimers having different edge-linkages—tris(hexadehydrotribenzo[12]annulene) (**2**) and tris(tetradehydrotribenzo[12]annulene) (**3**)—and three asterisk-shaped molecules, hexakis(phenylethynyl)benzenes (HPEB's), which have no edge linkage—hexakis(2,6-xylylethynyl)benzene (**4**), hexakis(phenylethynyl)benzene (**5**), and hexakis[(4-*tert*-butylphenyl)ethynyl]benzene (**6**)—in addition to [12]DBA itself (**1**).

The comparison of these compounds gives information on the effect of the edge-linkage due to the nature of the bonds—triple bond (**2**) vs double bond (**3**)—and in the no edge-linkage compounds the different degrees of freedom of the twisting motion of the peripheral phenyl rings are investigated (**4**–**6**). We introduced *tert*-butyl groups—which are electron donating groups—to **2** and **3** to improve the solubility. Thus, comparison of **2** and **3** with **6** is important to examine the effect of the edge linkage by ruling out the influence of the electron donating ability of the *tert*-butyl groups. In addition, the effect on length of the π-conjugate linker is discussed by comparing the [12]DBA-based compounds **1** and **2** (ethynylene linker) with the reported [18]DBA compounds (butadiynylene linker) having the same topology.

Another motivation for this study is a comparison with tetrakis(phenylethynyl)benzene (TPEB). HPEB's are a combination of three bis(phenylethynyl)benzene (BPEB) groups sharing the central phenyl ring. TPEB has this kind of combination with two BPEB's. The TPA property of the centrosymmetric TPEB compounds was reported previously.[14] On the other hand, the TPA property of HPEB's has never been reported although the third-order nonlinear optical property of the unsubstituted compound (**5**) was reported previously.[15] Therefore, the comparison between HPEB and TPEB gives information on the effect of the number and arrangement of the π-conjugated paths on TPA properties.

2. Results and Discussion

2.1 One-Photon Optical Properties

Absorption

Absorption bands for the compounds in chloroform are found in the blue-UV wavelength region (Figure 1). Some spectroscopic parameters obtained are summarized in Table 1. The trefoil-shaped compounds with different edge-linkage (**2** and **3**) exhibit similar spectra but **3** has broader peaks, suggesting the existence of various conformations or strong interaction with the solvent. The asterisk-shaped compounds (HPEB's) have rel-

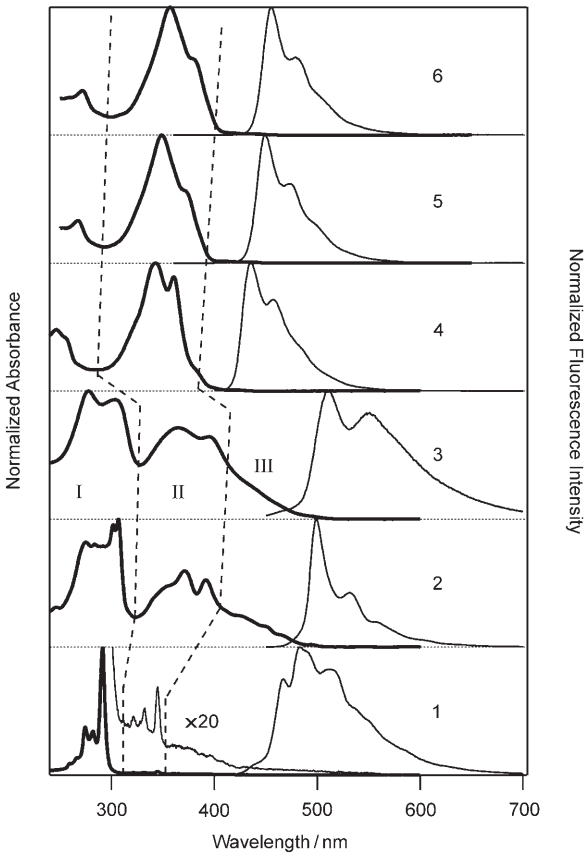

Figure 1. One-photon absorption (thick lines) and one-photon excited emission spectra (thin lines) in chloroform. The spectra are normalized at their maximum and are drawn with an offset by compound for clarity.

Table 1. One-photon optical properties of the compounds studied in chloroform.

Compound	λ_{abs} [nm][a]	ε_{max} [M^{-1} cm^{-1}][a]	λ_{em} [nm][b]	Φ_f[c]
1	344	7600	483	0.23
2	371	91000	499	0.23
3	369	54200	511	0.081
4	343	127000	435	0.20
5	349	144000	449	0.20
6	357	167000	455	N.A.

[a] At the absorption maximum in the wavelength range of 300–500 nm, [b] At the emission maximum, [c] Fluorescence quantum yield.

atively narrow absorption bands compared to the edge-linked compounds. The peak wavelength shifts slightly towards lower energy on going from **4** to **6**.

The observed absorption spectra can be divided into three regions: absorption bands observed at 310 nm or shorter wavelength (**I**), absorption bands observed around 310-400 nm (**II**), and the absorption tail which appears at longer wavelengths than Region **II** (**III**). The ratio of absorption intensities in Region **I** and Region **II** differs depending on the topology of the compounds. For the [12]DBA-based compounds (**1–3**), the absorption peaks in Region **I** are stronger than those in Region **II**. Particularly, for **1** the peaks in Region **I** are more intense than the peaks in Region **II**. This is due to the fact that the lowest-energy transition of one-photon absorption is symmetry forbidden for **1**.[4] Another characteristic feature of the [12]DBA-based compounds is a weak absorption tail in Region **III**. Contrary to this behaviour, for HPEB's (**4–6**), the absorption peaks in Region **I** are weaker than those in Region **II** and the absorption tail in Region **III** is negligible. From these facts, it is found that molecules having the diametrical π-conjugated path formed by the BPEB moiety (**2–6**) gain absorption intensity in Region **II**. On the other hand, gaining the absorption intensity in Region **I** and **III** is related to the triangular [12]DBA building unit. In particular, the appearance of the absorption band in Region **III** suggests that this band originates from the extension of π-conjugation by coupling between the conjugated paths along the edges of the triangle.

The absorption spectra of the [18]DBA-based molecules having the same topology as **1** and **2** were reported previously (see Figure 1 of ref. [11] and Figure 1 of the Supporting Information in ref. [12]). The absorption peak of the [18]DBA compounds blue-shifts by about 40 nm compared to that of **1** and **2**, due to the extra ethynyl group in each linker which extends the conjugation. However, one-to-one correspondence of each band is difficult because of the different spectral shapes. For unsubstituted [18]DBA, two prominent peaks in the region 350–370 nm are assigned to the forbidden transitions ($^1A_1' \rightarrow {}^1A_1'$ and $^1A_1' \rightarrow {}^1A_2'$ for a D_{3h} molecule) that gain intensity due to either vibronic coupling in the excited state or thermal motion in the ground state.[11] Compared to [18]DBA, [12]DBA is less flexible because of the short ethynylene linkage. Thus, the symmetry selection rules for the forbidden transitions are expected to hold more strictly for **1** and other [12]DBA compounds, compared to the [18]DBA compounds. This is a probable reason why the absorption band in Region **III** is relatively weak compared to the [18]DBA compounds.

Emission

All investigated compounds exhibit fluorescence under irradiation of UV light. Most of them have a fluorescence quantum yield of around 0.2, but that of **3** is approximately one third of the others (Table 1). The one-photon-excited emission spectra in chloroform, shown in Figure 1, all exhibit vibronic progressions. A characteristic feature of the [12]DBA-based compounds is the large Stokes shifts. This is probably related to the weak absorption band in Region **III** of the [12]DBA-based compounds.

2.2 Two-Photon Absorption Properties

Open-Aperture Z-Scan

Two-photon absorption spectra were first measured using the open-aperture Z-scan method. Compounds **1** and **3** do not give any nonlinear absorption (NLA) signal exceeding the noise level because of their low solubility or small cross section. On the other hand, **2**, **4**, **5**, **6** give prominent NLA signals. The recorded open-aperture traces were analyzed by the curve fitting assuming the TPA process.[16] Incident power-dependence of the obtained two-photon absorbance ($q_0 = \alpha^{(2)} I_0 L$ where $\alpha^{(2)}$ is the TPA coefficient, I_0 is the on-axis peak intensity at the focal point, and L is the path length) show a proportional relation for all compounds. Thus, the observed NLA can be assigned to the simultaneous TPA process. The obtained TPA cross-section spectra are shown in Figure 2. All spectra experience almost monotonic increase with decreasing wavelength, so the maximum values of the cross section are observed at the shortest wavelength. These values may not be peak values of the TPA bands; nevertheless they give valuable insights for their TPA properties. The values vary from 300 GM to 1300 GM depending on the compounds; however, these values are already significantly large as that of pure hydrocarbons[13] and are comparable to those of the [18]DBA compounds as mentioned later. The trefoil-type compound **2** has the largest value of all wavelengths and exhibits a sharp increase at wavelengths shorter than 600 nm. The maximum cross section obtained is 1300 ± 170 GM at 572 nm. The sharp increase in the short-wavelength region apparently resembles resonance enhancement.[16] However, the increase is unlikely to arise from the resonance enhancement because the one-photon absorption tail (~520 nm) is still far from the wavelength of the lowest-energy one-photon transition which is forbidden as discussed in Section 2.1. Thus, the sharp increase is assigned to an intense TPA peak located at 570 nm or shorter. Also a small

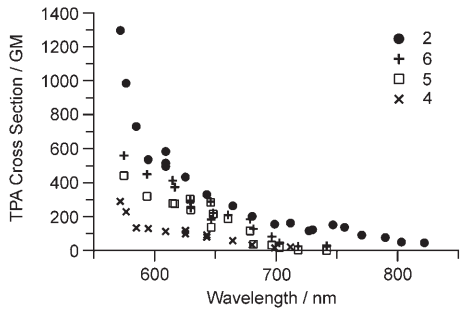

Figure 2. Two-photon absorption spectra of **2**, **4**, **5**, and **6** measured by the femtosecond open-aperture Z-scan method in chloroform. Experimental errors are approximately $\pm 15\%$.

peak is found at 750 nm although it is below the experimental error (approximately ±15%). These two TPA bands are characteristic of compound **2** and are not observed for **6**, which has the same molecular structure as **2** but no edge-linkage. The shape and magnitude of the other part of the TPA spectra are the same for **6** and **2**. Therefore, the two TPA bands characteristic of **2** must originate from the effect of the edge-linkage.

TPA cross sections of other HPEB's (**4** and **5**) are smaller than that of the *tert*-butyl derivative (**2**). The magnitude of the cross section decreases in the order of **6** > **5** > **4**. This order is understood qualitatively in terms of electron donating ability of substituent groups and steric hindrance induced by them. It is widely known that introducing electron donating groups at both ends of a π-conjugated chain enhances the TPA activity of the molecule.[17] The *tert*-butyl groups in *para* positions of the peripheral phenyl rings act as donors and the enhancement occurs along three conjugate paths in the diameter direction for **6**. Thus, it is reasonable that **6** exhibits larger TPA activity than **5**. Meanwhile, the peripheral phenyl rings of **4** cannot be parallel to the central phenyl ring due to the steric hindrance of the *ortho*-methyl groups. This reduces the extent of π-conjugation of the conjugated path along the diametrical direction for **4**, resulting in the small TPA activity compared to the unsubstituted HPEB (**5**).

Two-Photon-Induced Fluorescence Measurements

We also performed TPIF experiments to obtain TPA spectra of **1** and **3**, which could not be observed by the Z-scan method due to the sensitivity limit. Compound **2** acts as a reference and is measured at the same time (the values of the TPA cross section of **2** obtained from the open-aperture Z-scan methods are used for scaling). The obtained spectra of **1** and **3** together with **2** are shown in Figure 3.

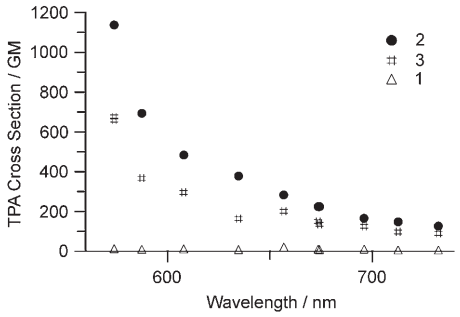

Figure 3. Two-photon absorption spectra of **1** and **3** in chloroform measured by two-photon-induced fluorescence measurements with the same femtosecond laser used for the Z-scan measurements. Compound **2** is measured as reference and those values obtained from the Z-scan method are used for vertical scaling. Experimental errors are approximately ±15%.

The TPA spectrum of **3** is similar to that of **2**. The spectrum has a strong TPA band at wavelengths shorter than 600 nm and considerable TPA intensity at wavelengths longer than 700 nm where HPEB's have no intensity at all. These features are in common for the edge-linked compounds (**2** and **3**). Thus, the TPA bands probably originate from the electron coupling through the edge-linkage. The maximum value of the cross section of **3** is 670 ± 100 GM at 574 nm. This value is almost half of that of **2**. This result contradicts the previous reports that vinylene groups give higher TPA cross sections than ethynylene groups because of their stronger π-conjugation.[18,19] However, the vinylene-linkage induces strain in the [12]DBA fragment of **3**. It was also reported that the vinylene-linkage rotates rapidly to exhibit a single ^{1}H NMR signal for the two vinyl protons which are otherwise not equivalent.[20] Therefore, the peripheral phenyl rings of **3** which deviate from the planar structure compared to those of **2**, yield a small cross section.

On the other hand, the TPA cross section of the repeating unit molecule (**1**) is found to be less than 10 GM, which is, nearly one order or more, smaller than that of the others. This clearly shows the importance of the long conjugated path along the diametric direction for high TPA cross section.

2.3 Controlling Factors of the TPA Cross Section

From the results of the Z-scan and TPIF measurements, the TPA cross section of the compounds studied follows the order of **2** > **3** ~ **6** ≥ **5** > **4** ≫ **1**. Clearly, the cross section differs by one order of magnitude or more depending on the molecules having the diametric π-conjugated paths (**2–6**) or not (**1**). This suggests that the diametric π-conjugated paths are of primary importance for large TPA cross sections.

The next factor to determine this order is planarity of the molecule. The higher the planarity, the larger the extent of the π-conjugation—which results in a stronger TPA. The ethynylene-linked, trefoil-shaped compound **2** exhibits the largest cross section of all. The molecular structure of **2** is considered to be virtually planar and the most rigid although it is predicted to have a propeller-shape structure with a small skewing angle.[8–9] Meanwhile, the others have some degrees of rotational freedom. As mentioned above, the vinylene-linkage of **3** is known to rotate rapidly. Rotational motion of the peripheral phenyl groups of **5** and **6** can also be activated thermally because of the small barrier height of the rotational motion of diphenylacetylene around the triple bond (2.4 kJ mol^{-1}), which is comparable to the thermal activation energy at room temperature (kTN_A = 2.5 kJ mol^{-1} at T = 297 K).[21] Thus, various rotational conformers can exist in solution which results in a smaller cross section. Moreover, the steric hindrance between the *ortho*-methyl groups of **4** prevents the molecule taking the planar structure, resulting in a smaller cross section than others. The effect of the electron-donating ability of the peripheral substituents results in compound **6** having a higher TPA cross section than **5**. Although the methyl side groups of **4** can also act as an electron donor, the effect is overcome by the negative effect arising from the steric hindrance.

The above discussions can be applied to the magnitude of the cross sections in the broad spectral region from 600 nm to 700 nm. However, the edge-linked molecules exhibit characteristic TPA bands that cannot be explained through planarity.

The bands are located outside the 600–700 nm range. The TPA band observed at the shorter wavelength is particularly important because the maximum TPA cross section of **2** and **3** are observed in this band. These TPA bands are related to the electronic coupling of π-conjugated paths between the diametric and the edge-linked directions. However, further studies are needed to clarify the nature of the TPA bands and how they relate with the electronic coupling.

It is worth noting that the observed TPA cross section of the [12]DBA-based compounds are almost the same as the reported values of the [18]DBA-based compounds. The maximum TPA cross section of **2** is observed to be 1300 GM (at 572 nm) and that of the corresponding [18]DBA compound having the same topology was reported to be 1346 GM (at 765 nm).[12] Also that of **1** is observed to be 7 GM (at 574 nm) and that of the corresponding [18]DBA was reported to be 11.5 GM.[12] This result has two important implications: one is that the large values of TPA cross section over 1000 GM is confirmed for the hydrocarbon without strong donor/acceptor system; and the other is that it introduces the question of why the cross sections are the same magnitude in spite of the difference in the π-conjugation length? The [18]DBA compounds have a longer π-conjugated path, with an extra ethynyl group, than the [12]DBA compounds; so a larger cross section is expected for the [18]DBA compounds. Indeed, the larger cross section is observed with the longer conjugated arm for the tri-branched structure.[22,23] The TPA peak red-shifts by almost 200 nm from the [12]DBA (**2**) to the [18]DBA. This large red shift is more than that expected from the red shift of the one-photon absorption peak [390 nm for **2** and 442 nm for the corresponding [18]DBA compound (see Supporting Information of ref. [12])]. This suggests that the energy level of the final (A_1') state of the TPA transition is largely lowered, compared to those of other one-photon allowed (E') excited states, with lengthening of the π-conjugation linkers. However, a reasonable explanation cannot be given to date, for the reasons why the peak TPA cross sections are almost the same and why the energy level of the TPA-allowed excited state is so different between the [12]DBA and [18]DBA compounds. Clearly, further studies on their electronic structures are needed and detailed quantum chemical calculations of the excited states are in progress.

Another intriguing problem is the relationship between the TPA property and the number of the diametric conjugated paths. The present results show that for HPEB, in which three diametric π-conjugated paths of BPEB cross at the central phenyl ring, a large TPA cross section in the order of several hundreds GM's is obtained. It was reported that the TPA of "one" conjugated path is negligibly small,[12] however Slepkov and co-workers reported that dimethylamino-substituted TPEB—which consists of two crossing conjugated paths—has a peak TPA cross section of 520 GM at 710 nm.[14] This value is comparable to the maximum value of **6** (560 GM at 575 nm). Thus, augmentation with one more conjugated path effectively increases the TPA cross section, at least, to the same extent as the effect of a strong donor. However, the peak wavelengths are quite different to each other. Further comparative studies are also needed with the same substituent groups.

3. Conclusions

Herein, the TPA properties of [12]DBA, two [12]DBA-based, trefoil-shaped compounds with different edge-linkages, and three HPEB's with different substituents were studied experimentally by the open-aperture Z-scan and TPIF methods. It is found that 1) the HPEB structure gives relatively high TPA cross sections of several hundred GM's over a broad spectral region. The relative intensities among the HPEB's with different end substituents (**4**–**6**) can be explained by the planarity in relation to the steric hindrance and the electron-donating ability of the end substituent groups. 2) the edge-linkage is found to enhance the TPA in some specific bands by promoting coupling of the π-conjugated paths. The significantly high cross section over 1000 GM was recorded at the TPA band.

Contrary to the previous conclusion that high symmetry is the dominant factor for high TPA activity,[12] we now conclude that the length and the number of the conjugated paths in a molecule determines the cross section. The number of the long-conjugated paths determines the approximate magnitude of the TPA cross section, and when the conjugated paths are interconnected through the edge-linkage an intense TPA band is observed.

Experimental Section

Chemicals: Compounds **1**[24], **2**[8], **3**[8], and **5**[25] were prepared according to literature procedures. These compounds were purified by re-crystallization from the following solvents: hexane for **1**, $CHCl_3$ for **2** and **3**, and THF for **5**.

Hexakis(2,6-xylylethynyl)benzene (**4**): Under a nitrogen atmosphere, 1-ethynyl-2,6-dimetylbenzene (172 mg, 1.32 mmol) was dissolved in THF (4 mL), and cooled to −78 °C. BuLi (1.56 M in hexane, 0.85 mL, 1.33 mmol) was added dropwise via a syringe over 15 min. After 30 min, a THF (4 mL) solution of $ZnCl_2$ (179 mg, 1.33 mmol) was added and the mixture was stirred for 30 min at −78 °C before it was warmed to room temperature. The mixture was then added via a syringe to a toluene solution (2 mL) of hexabromobenzene (61.1 mg, 0.111 mmol) and $Pd(PPh_3)_4$ (38.9 mg, 33.7 μmol). After stirring for 48 h at 80 °C, the reaction was quenched with a small amount of $HCl_{(aq)}$. The mixture was diluted with $CHCl_3$, and the organic layer was washed with $HCl_{(aq)}$ and brine, and dried over $MgSO_4$. The $CHCl_3$ solution was passed through a short silica-gel column, and the solvent was evaporated under vacuum. Silica-gel column chromatography (hexane/toluene = 3/1 as an eluent) and re-crystallization from $CHCl_3$ gave **4** (28 mg, 30% yield) as a yellow solid. mp 286–287 °C; ^{1}H NMR (270 MHz, $CDCl_3$) δ = 7.12–7.07 (m, 6H), 6.98–6.96 (m, 12H), 2.33 ppm (s, 36H); ^{13}C NMR (67.5 MHz, $CDCl_3$) δ = 140.8, 128.1, 127.9, 126.5, 123.0, 96.9, 95.3, 21.1 ppm; IR (KBr) 3019, 2922, 2201, 1636, 1467, 768, 670 cm^{-1}; MS (FAB) *m/z* 846 (M^+).

Hexakis[(4-*tert*-butylphenyl)ethynyl]benzene (**6**): Hexabromobenzene (551 mg, 1.00 mmol), $Pd(PPh_3)_4$ (116 mg, 0.100 mmol), and CuI (40 mg, 0.20 mmol) were suspended in Et_3N (5 mL) and DMSO (2 mL) under a nitrogen atmosphere. 4-*tert*-Butyl-1-ethynylbenzene (1.59 g, 10.0 mmol) was added to the above mixture. After stirring for 24 h at 60 °C, the volatile solvent was removed under vacuum. Resulting mixture was passed through a short column of silica-gel ($CHCl_3$ as an eluent). Purification was performed with silica-gel column chromatography (hexane:$CHCl_3$ = 7:3 as an eluent) fol-

lowed by re-crystallization from hexane/$CHCl_3$ (6:4) to give **6** (120 mg, 12% yield) as yellow needles. mp 310 °C (decomposition); ^{1}H NMR (300 MHz, $CDCl_3$) δ = 7.61–7.54 (m, 12H), 7.42–7.34 (m, 12H), 1.35 ppm (s, 54H); ^{13}C NMR (75 MHz, $CDCl_3$) δ = 151.9, 131.5, 127.3, 125.3, 120.3, 99.3, 87.1, 35.0, 31.3 ppm; IR (KBr) 3039, 2962, 2866, 2209, 1664, 1506, 1361, 1268, 1106, 896 cm^{-1}; high-resolution mass spectroscopy (FAB) calcd. for $C_{78}H_{78}$ 1014.6104, found 1014.6094.

Optical Experiments: One-photon absorption and one-photon excited emission spectra of the compounds were recorded by commercial spectrophotometers (Shimadzu UV-3150 and Hitachi F-4500, respectively). Fluorescence quantum yield was determined with reference to rhodamine B (Φ_f = 0.69)[26] for a low (1.4×10^{-6} M) concentration solution in ethanol. The spectral shapes of one-photon absorption of the compounds are unchanged for the concentration range from 10^{-6} to 10^{-3} M. Thus, the effect of aggregation is ignored for the Z-scan and TPIF measurements.

TPA of the compounds was measured by the open aperture Z-scan and TPIF methods. An optical parametric amplifier (Spectra-Physics OPA-800) was used as the light source (pulse duration: 130 fs, repetition rate was 1 kHz). The details of the Z-scan setup and the analysis were reported previously.[16,27] All compounds were dissolved in spectroscopic grade chloroform. The concentrations of the sample solutions were 9.9 mM for **1**, 1.1 mM for **2**, 0.16 mM for **3** (saturated), 2.8 mM for **4**, 1.4 mM for **5** (saturated), and 5.4 mM for **6**. The Rayleigh range was twice or more as long as the pathlength (2 mm). The on-axis peak intensity of the laser pulse was varied from 50 to 500 GW cm^{-2}.

The TPIF experiments were performed with emission-collection optics attached to the Z-scan setup. A four-sided quartz cuvette (2 mm pathlength in one direction) was used for the sample cell. The cuvette was placed at the focal point of the laser beam and was oriented so that the laser beam passes along the direction of the 2 mm pathlength. The emission was collected by an objective lens (×20) whose optical axis was perpendicular to the laser beam. In order to minimize the influence of reabsorption of the emission, the illumination spot of the laser beam was adjusted as close as possible (less than 1 mm away) to the cell wall facing the objective lens. The collimated emission was fiber-coupled and then detected by a polychromator (Ocean Optic USB-2000). The recorded emission spectrum was corrected by using calibration data obtained by the calibrated fluorescence spectrometer (Hitachi F-4500). The quadratic dependence of the emission on the incident power was confirmed for each measurement.

The integrated fluorescence intensity $S = \int I_f(\lambda)d\lambda$ is related to the two-photon transition rate as given in Equation (1):[28]

$$S = \frac{1}{2} C g^{(2)} \Phi_f \sigma^{(2)} N F^2 \quad (1)$$

where C is the collection efficiency of the two-photon emission, $g^{(2)}$ is the second-order coherence, $\sigma^{(2)}$ is the TPA cross section, N is the number density of the molecule to be measured, and F is the photon flux. By keeping the experimental conditions constant during the measurement, $Cg^{(2)}F^2$ is constant and only $\Phi_f\ \sigma^{(2)}N$ varies from a sample to another. Therefore, the TPA cross section of the sample molecule can be obtained as Equation (2):

$$\sigma_s^{(2)} = \frac{\Phi_{f,r} N_r S_s}{\Phi_{f,s} N_s S_r} \sigma_r^{(2)} \quad (2)$$

Here subscripts s and r refer to the sample and reference, respectively. For the consistency with the result of the Z-scan experiments, the values of the cross section obtained by the Z-scan measurements was used for the reference value $\sigma_r^{(2)}$.

The Rayleigh range and other optical conditions for the TPIF measurements are the same as those for the Z-scan measurements. The on-axis peak intensity was approximately 100 GW cm^{-2} or less. The solvent used for the TPIF measurement is spectroscopic-grade chloroform for all samples. Lower concentrations than those for the Z-scan measurements were used (0.30 mM for **1**, 0.08 mM for **2**, and 0.16 mM for **3**).

Acknowledgements

LA thanks the Japan Society for the Promotion of Science for a fellowship.

Keywords: aromatic compound · electronic coupling · fluorescence · hydrocarbons · two-photon absorption

[1] R. H. Baughman, H. Eckhardt, M. J. Kertesz, *J. Chem. Phys.* **1987**, *87*, 6687–6699.
[2] N. Narita, S. Nagai, S. Suzuki, K. Nakano, *Phys. Rev. B* **1998**, *58*, 11009–11014.
[3] N. Narita, S. Nagai, S. Suzuki, K. Nakano, *Phys. Rev. B* **2000**, *62*, 11146–11151.
[4] J. Wirz, *Excited States in Organic Chemistry and Biology*, (Eds: B. Pullman and N. Goldblum), Reidal Publishing Company, Dordrecht, **1977**, 283.
[5] A. Sarkar, J. J. Pak, G. W. Rayfield, M. M. Haley, *J. Mater. Chem.* **2001**, *11*, 2943–2945.
[6] J. M. Kehoe, J. H. Kiley, J. J. English, C. A. Johnson, R. C. Petersen, M. M. Haley, *Org. Lett.* **2000**, *2*, 969–972.
[7] M. Sonoda, Y. Sakai, T. Yoshimura, Y. Tobe, K. Kamada, *Chem. Lett.* **2004**, *33*, 972–973.
[8] T. Yoshimura, A. Inaba, M. Sonoda, K. Tahara, Y. Tobe, R. V. Williams, *Org. Lett.* **2006**, 8, 2933–2936.
[9] K. Tahara, T. Yoshimura, M. Sonoda, Y. Tobe, R. V. Williams, J. Org. Chem. 2007, *72*, 1437–1442.
[10] W. B. Wan, S. C. Brand, J. J. Pak, M. M. Haley, *Chem. Eur. J.* **2000**, *6*, 2044–2052.
[11] S. Anand, O. Varnavski, J. A. Marsden, M. M. Haley, H. B. Schlegel, T. Goodson, III, *J. Phys. Chem. A* **2006**, *110*, 1305–1318.
[12] A. Bhaskar, R. Guda, M. M. Haley, T. Goodson, III, *J. Am. Chem. Soc.* **2006**, *128*, 13972–13973.
[13] K. Kamada, K. Ohta, T. Kubo, A. Shimizu, Y. Morita, K. Nakasuji, R. Kishi, S. Ohta, S. Furukawa, H. Takahashi, M. Nakano, *Angew. Chem.* **2007**, *119*, 3614–3616.
[14] A. D. Slepkov, F. A. Hegmann, R. R. Tykwinski, K. Kamada, K. Ohta, J. A. Marsden, E. L. Spitler, J. J. Miller, M. M. Haley, *Opt. Lett.* **2006**, *31*, 3315–3317.
[15] K. Kondo, S. Yasuda, T. Sakagushi, M. Miya, *J. Chem. Soc., Chem. Commun.* **1995**, 55–56.
[16] K. Kamada, K. Ohta, Y. Iwase, K. Kondo, *Chem. Phys. Lett.* **2003**, *372*, 386–393.
[17] M. Albota, D. Beljonne, J.-L. Brédas, J. E. Ehrlich, J.-Y. Fu, A. A. Heikal, S. E. Hess, T. Kogej, M. D. Levin, S. R. Marder, D. McCord-Maughon, J. W. Perry, H. Röckel, M. Rumi, G. Subramaniam, W. W. Webb, X.-L. Wu, C. Xu, *Science* **1998**, *281*, 1653–1656.
[18] M. G. Silly, L. Porrés, O. Mongin, P.-A. Chollet, M. Blanchard-Desce, *Chem. Phys. Lett.* **2003**, *379*, 74–80.
[19] S. Kato, T. Matsumoto, M. Shigeiwa, H. Gorohmaru, S. Maeda, T. Ishi-i, S. Mataka, *Chem. E. J.* **2006**, *12*, 2303–2317.
[20] H. A. Staab, R. Bader, *Chem. Ber.* **1970**, *103*, 1157–1167.
[21] K. Okuyama, T. Hasegawa, M. Ito, N. Mikami, *J. Phys. Chem.* **1984**, *88*, 1711–1716.
[22] C. Le Droumaguet, O. Mongin, M. H. V. Werts, M. Blanchard-Desce, *Chem. Commun.* **2005**, 2802–2804.

[23] F. Terenziani, C. Le Droumaguet, C. Katan, O. Mongin, M. Blanchard-Desce, *ChemPhysChem* **2007**, *8*, 723–734.
[24] H. A. Staab, F. Graf, *Tetrahedron Lett.* **1966**, *7*, 751–757; C. Huynh, G. Linstrumelle, *Tetrahedron* **1988**, *44*, 6337–6344.
[25] W. Tao, S. Nesbitt, R. F. Heck, *J. Org. Chem.* **1990**, *55*, 63–69.
[26] J. F. Rabek, *Experimental Methods in Photochemistry and Photophysics* (Part 2), John Wiley & Sons, Chichester, **1982**, 751.
[27] L. Antonov, K. Kamada, K. Ohta, F. S. Kamounah, *Phys. Chem. Chem. Phys.* **2003**, *5*, 1193–1197.
[28] C. Xu, W. W. Webb, *J. Opt. Soc., Am. B* **1996**, *13*, 481–491.

Received: August 14, 2007
Revised: October 1, 2007
Published online on November 14, 2007

